A Novel PAPR Reduction Scheme for SC-OFDM with Frequency Domain Multiplexed Pilots

Fumihiro Hasegawa, Akihiro Okazaki, Hiroshi Kubo, Damien Castelain, and David Mottier

***Abstract*—In this letter, a novel data-pilot multiplexing scheme with reduced peak to average power ratio (PAPR) is introduced for single carrier (SC)-orthogonal frequency division multiplexing (OFDM) systems. In the proposed scheme, phases of SC-OFDM symbols are rotated adaptively such that PAPR is reduced and circular shifts are introduced in the time domain (TD). To index the amount of phase rotation applied at the transmitter, a sequence of pilot symbols, which is unique for each phase rotation angle, is chosen from a predetermined set and multiplexed with the phase rotated SC-OFDM symbols in the frequency domain. Simulation results indicate that the proposed method can reduce the PAPR dramatically, and yield superior bit error rate (BER) performance compared to conventional methods.**

***Index Terms*—SC-FDE, SC-OFDM, PAPR, adaptive techniques.**

I. Introduction

SINGLE CARRIER-orthogonal frequency division multiplexing (OFDM) is an attractive transmission method due to its low peak power and robust performance against multipath fading channels [1]. To achieve frequent channel estimation in fast fading environments, pilot symbols need to be multiplexed with discrete Fourier transform (DFT)-precoded symbols in single carrier (SC)-frequency domain equalization (FDE) systems[1]. However, insertion of pilot symbols in a SC-OFDM symbol destroys its single carrier property, causing the peak to average power ratio (PAPR) to increase [2].

To overcome the problem, the authors in [2] proposed an adaptive hybrid SC-OFDM transmission method, namely frequency domain superimposed pilot technique (FDSPT). The disadvantage of the FDSPT is the penalty on bit error rate (BER) performance due to the superimposition of DFT precoded symbols with pilot symbols. Proposals to improve the BER performance of FDSPT exist [3] [4] but the proposed methods require additional computations at both transmitters and receivers to minimize the BER performance degradation. Moreover, the methods in [3] [4] are not optimized to minimize the PAPR of data-pilot multiplexed SC-OFDM symbols.

In this letter, a novel PAPR minimizing adaptive hybrid (A-Hyb) SC-OFDM transmission method is proposed. Unlike FDSPT which utilizes pilot symbols to lower the peak transmission power, the proposed method applies phase rotation to data symbols in frequency domain (FD) to minimize the PAPR. A sequence of pilot symbols chosen uniquely for each phase rotation angle is inserted at predetermined positions in FD to index the phase rotation angle applied at the transmitter. The pilot symbols used in this letter are chosen from a predetermined set. The receiver then determines the phase rotation angle applied at the transmitter by identifying the transmitted pilot sequence.

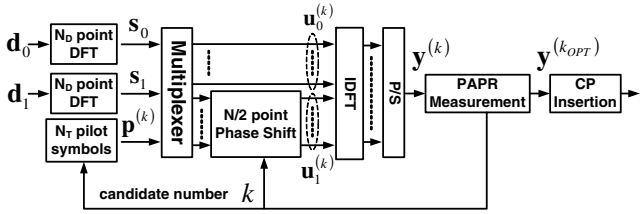

Fig. 1. Block diagram of the proposed A-Hyb SC-OFDM transmitter.

II. Proposed Hybrid SC-OFDM Transmission

A block diagram of the proposed A-Hyb transmitter is shown in Fig. 1. In the proposed scheme, two groups of N_D information symbols $\mathbf{d}_0$ and $\mathbf{d}_1$ are precoded by N_D-point DFT to create two sets of SC-OFDM symbols, $\mathbf{s}_n = [s_{0,n}, s_{1,n}, \cdots, s_{N_D-1,n}]^T = \mathbf{W}_{N_D}\mathbf{d}_n$ where the $(k,l)^{th}$ element of $N_D \times N_D$ DFT precoding matrix $\mathbf{W}_{N_D}$ is given by $[\mathbf{W}_{N_D}]_{k,l} = \frac{1}{\sqrt{N_D}} e^{-j2\pi kl/N_D}$ and $E\left[|s_{j,n}|^2\right] = E_S$. The m^{th} precoded symbol in the n^{th} group is denoted by $s_{m,n}$ with $0 \le m \le N_D - 1$ and $0 \le n \le 1$. Following the DFT operation, a pilot sequence which consists of N_T pilot symbols is multiplexed with precoded data symbols to create a hybrid SC-OFDM symbol. The Chu sequence [5] with circular shifts $a^{(k)}$,

$$p_m^{(k)} = e^{j\pi\left(\mathrm{mod}_{(m-a^{(k)},N_T)}\right)^2/N_T}, \tag{1}$$

is used as the pilot sequence $\mathbf{p}^{(k)} = \left[p_0^{(k)}, p_1^{(k)}, \ldots, p_{N_T-1}^{(k)}\right]^T$ for the k^{th} phase rotation candidate, where the modulo operation is denoted as $\mathrm{mod}(\cdot)$. There are $N = 2N_D + N_T$ symbols in a data frame where N is assumed to be an even number and divisible by N_T. The phase rotation is performed after the insertion of pilot symbols. As shown in Fig. 2, the pilot symbols are placed in FD at indices $I_P = \{0, P_D, 2P_D, \ldots, (N_T-1)P_D\}$ with $P_D = N/N_T$, and the hybrid symbols are separated by T_D data symbols in the time domain (TD).

Manuscript received March 5, 2012. The associate editor coordinating the review of this letter and approving it for publication was M. Tao.

F. Hasegawa and A. Okazaki are with Mitsubishi Electric Corporation, Information Technology R & D Center, Kamakura, Kanagawa 247-8501, Japan (e-mail: Hasegawa.Fumihiro@bk.MitsubishiElectric.co.jp).

H. Kubo was with Mitsubishi Electric Corporation. He is presently with Ritsumeikan University, Department of Electronics and Information Engineering, Kusatsu, Shiga 525-8577, Japan.

D. Castelain and D. Mottier are with Mitsubishi Electric R&D Centre Europe, CS 10806, 35708 Rennes Cedex 7, France.

Digital Object Identifier 10.1109/LCOMM.2012.12.120474

[1]In this letter, a group of DFT precoded symbols is referred to as a "SC-OFDM" symbol.

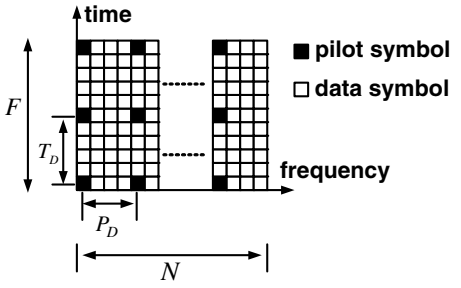

Fig. 2. Frame structure.

In this letter, the k^{th} phase rotation candidate is defined as $\psi_n^{(k)}$ where $\psi_0^{(k)} = 0$ is assumed for simplicity. The phase rotated symbols multiplexed with pilot symbols $\mathbf{u}_n^{(k)} = \left[u_{0,n}^{(k)}, \cdots, u_{N/2-1,n}^{(k)}\right]^T$ are defined as

$$u_{m,n}^{(k)} = \begin{cases} p_{m+n\cdot N_T/2}^{(k)} & m + n \cdot N/2 \in I_P \\ s_{m',n} \cdot \theta_{m,n}^{(k)} & \text{otherwise} \end{cases} \quad (2)$$

for $0 \le m \le N/2-1$ with $\theta_{m,n}^{(k)} = e^{j2\pi m \psi_n^{(k)}/(N/2)}$ and $m' := m - \lfloor m/P_D \rfloor - 1$. If phase rotated symbols are denoted as $s_{m',n}^{(k)} = s_{m',n} \cdot \theta_{m,n}^{(k)}$ with $\theta_{m,0}^{(k)} = 1$ for $0 \le m \le N/2-1$, the hybrid SC-OFDM symbol in FD for the k^{th} phase rotation candidate can be represented as

$$\mathbf{v}^{(k)} = \left[p_0^{(k)}, s_{0,0}^{(k)}, \ldots, s_{N_D-1,0}^{(k)}, p_{N_T/2}^{(k)}, \ldots, s_{N_D-1,1}^{(k)}\right]^T. \quad (3)$$

Let us define the PAPR as $X^{(k)} = \frac{\max\left|y_n^{(k)}\right|^2}{E\left[\left|y_n^{(k)}\right|^2\right]}$ for $0 \le n \le L_{OS} \cdot N - 1$ where L_{OS} denotes the oversampling rate and $y_n^{(k)}$ is the time-domain signal of $\mathbf{v}^{(k)}$ in (3). Then, the normalized phase rotation angle $\psi_1^{(k)}$ that minimizes the PAPR is chosen as $k_{OPT} = \arg\min_{0\le k\le C-1} X^{(k)}$ where C is the number of phase rotation angle candidates. After insertion of the length-N_{CP} cyclic prefix (CP), $\mathbf{y}^{(k_{OPT})}$ is transmitted where $\mathbf{y}^{(k_{OPT})} = \left[y_0^{(k_{OPT})}, y_1^{(k_{OPT})}, \cdots, y_{N-1}^{(k_{OPT})}\right]^T$ is the optimized time-domain signal.

Let us denote the $N \times N$ inverse discrete Fourier transform (IDFT) matrix $\mathbf{W}_N^H$, diagonal phase rotation matrix $\Phi^{(k)} = \text{diag}\left\{\left[\theta_{0,1}^{(k)}, \ldots, \theta_{N_D-1,1}^{(k)}\right]\right\}$, $N \times N_D$ data symbol placement matrix

$$[\mathbf{P}_n]_{k,l} = \begin{cases} 1 & k \notin I_P, l = k - \lfloor k/P_D \rfloor - 1 \\ 0 & \text{otherwise} \end{cases} \quad (4)$$

with $n \cdot N/2 \le k \le (n+1)\cdot N/2 - 1$ and $N \times N_P$, and pilot symbol placement matrix

$$[\mathbf{Q}]_{k,l} = \begin{cases} 1 & k \in I_P, l = \lfloor k/P_D \rfloor \\ 0 & \text{otherwise} \end{cases} \quad (5)$$

Then $\mathbf{y}^{(k)}$ can be written as

$$\mathbf{y}^{(k)} = \mathbf{W}_N^H \left(\underbrace{\mathbf{P}_1 \Phi^{(k)} \mathbf{W}_{N_D}}_{\mathbf{x}_1^{(k)}} \mathbf{d}_1 + \underbrace{\mathbf{P}_0 \mathbf{W}_{N_D}}_{\mathbf{x}_0} \mathbf{d}_0 + \mathbf{Q}\mathbf{p}^{(k)} \right) \quad (6)$$

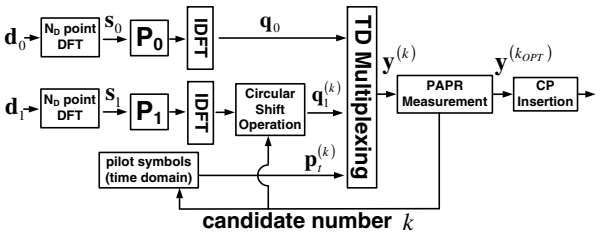

Fig. 3. Time domain representation of A-Hyb transmitter.

If normalized phase rotation angles are chosen as

$$\psi_n^{(k)} = \phi^{(k)}/2 \quad (7)$$

for $\phi^{(k)} = 0, \pm1, \pm2, \cdots$, it can be shown that the m^{th} row of $\mathbf{W}_N^H \mathbf{X}_1^{(k)}$ is given by

$$\left[\mathbf{W}_N^H \mathbf{X}_1^{(k)}\right]_m = (-1)^m \cdot \left[\mathbf{W}_N^H \mathbf{X}_0\right]_{\text{mod}(m+\phi^{(k)},N)}. \quad (8)$$

Let us define the following TD signals, $\mathbf{q}_0 = \mathbf{W}_N^H \mathbf{P}_0 \mathbf{W}_{N_D} \mathbf{d}_0$, $\mathbf{p}_t^{(k)} = \mathbf{W}_N^H \mathbf{Q}\mathbf{p}^{(k)}$ and $\mathbf{q}_1^{(k)} = \mathbf{W}_N^H \mathbf{P}_1 \Phi^{(k)} \mathbf{W}_{N_D} \mathbf{d}_1$. It is clear from (8) that the phase rotation angle in (7) creates a circular shift in $\mathbf{q}_1^{(k)}$. Thus, the goal in the proposed method is to find a phase rotation angle that introduces a circular shift in $\mathbf{q}_1^{(k)}$ so that a peak location in $\mathbf{q}_1^{(k)}$ is aligned with a peak-cancelling location of $\mathbf{q}_0$, or vice versa, resulting in destructive interference. To illustrate the time-frequency duality, a TD model of the proposed A-Hyb transmitter in Fig. 1 is depicted in Fig. 3.

As an example, the real and imaginary part of $\mathbf{q}_0$, $\mathbf{q}_1^{(k)}$ and $\mathbf{p}_t^{(k)}$, and $|y_m^{(k)}|$ are shown in Fig. 4 when $N = 32$, $N_D = 12$, $N_T = 8$, $L_{OS} = 4$, $\phi^{(k)} \in \{0, +1, -1, +2, -2\}$, and $a^{(k)} \in \{0, 1, 2, 3, 4\}$. The received signal with and without circular shifts are shown in Fig. 4 (a) and (b), respectively. From Fig. 4 (a), it is apparent by observing $|y_m^{(0)}|$ that the peak is located at $m = 29$. However, it is evident from $|y_m^{(4)}|$ in Fig. 4 (b) that PAPR reduction is achieved since the real part of the peak location of $\mathbf{q}_1^{(0)}$ at $m = 29$ is aligned with peak-cancelling portion of $\mathbf{q}_0$ when $k = 4$.

III. Reception Method

In this letter, a Rayleigh frequency selective channel model $f(t) = \sum_{l=0}^{L-1} h_l \delta(t - lT_C)$ is considered where $T_S = N \cdot T_C$, $\delta(\cdot)$ and L denote the SC-OFDM symbol duration, delta function and number of multipaths, respectively. It is assumed that the channel remains constant during one SC-OFDM symbol interval and $E[h_l \cdot h_m^*] = \delta(l-m)$ for $\forall l, m$ where the asterisk denotes the complex conjugate. The channel state information (CSI) in FD is related to the CSI in TD by $\mathbf{f} = \mathbf{W}_{N,L}\mathbf{h}$ where $\mathbf{h} = [h_0, \cdots, h_{L-1}]^T$, $\mathbf{f} = [f_0, \cdots, f_{N-1}]^T$ and $[\mathbf{W}_{N,L}]_{l,k} = e^{j2\pi lk/N}$ [6]. The received signal in FD can be represented by $r_m = f_m \cdot v_m^{(k_{OPT})} + w_m$ where $\mathbf{v}^{(k_{OPT})} = \left[v_0^{(k_{OPT})}, \cdots, v_{N-1}^{(k_{OPT})}\right]^T$ and w_m is additive white Gaussian noise (AWGN) with $E\left[|w_m|^2\right] = \sigma_w^2$. A vector of received signals corresponding to pilot indices can be written as $\mathbf{r}_P = \left[r_0, r_{P_D}, \cdots, r_{(N_T-1)P_D}\right]^T$. Using $\mathbf{r}_P$, an estimate of the received signal for the k^{th} pilot sequence can be obtained

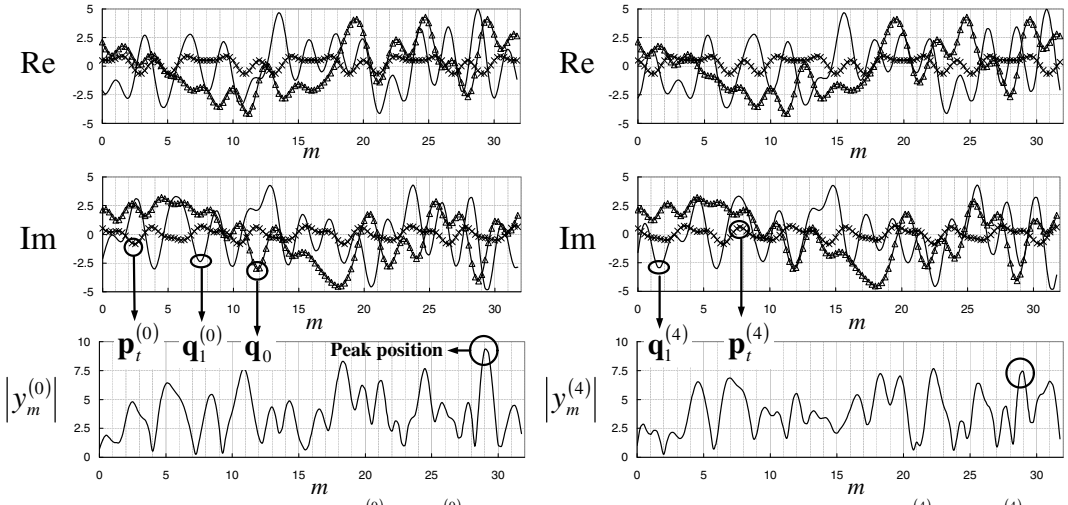

Fig. 4. PAPR minimization with circular shift: real and imaginary part of $q_1^{(k)}$, $p_t^{(k)}$ and q_0 are represented by solid line, "×" and "Δ", respectively.

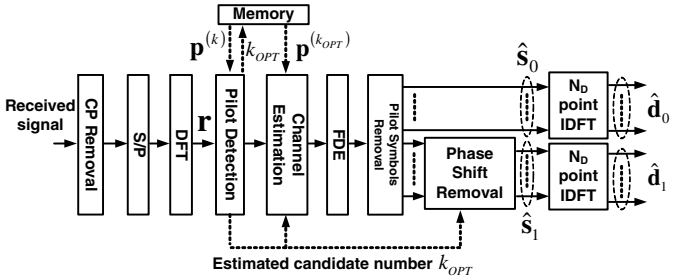

Fig. 5. Block diagram of the proposed receiver.

TABLE I
PARAMETER TABLE FOR A-HYB AND FDSPT

	k	0	1	2	3	4
$C = 3$	$a^{(k)}$	0	2	4	-	-
	$\phi^{(k)}$	0	$+1$	-1	-	-
$C = 5$	$a^{(k)}$	0	2	4	6	8
	$\phi^{(k)}$	0	$+1$	-1	$+2$	-2

with $\hat{\mathbf{r}}_P^{(k)} = \mathbf{W}_P \left(\mathbf{W}_P^H \mathbf{W}_P\right)^{-1} \mathbf{W}_P^H \mathbf{S}_P^{(k)H} \mathbf{r}_P$, where $\mathbf{W}_P$ can be obtained by extracting rows with indices I_P from $\mathbf{W}_{N,L}$, and $\mathbf{S}_P^{(k)} = \mathrm{diag}\{\mathbf{p}^{(k)}\}$. The transmitted pilot sequence can be detected as $k_{OPT} = \arg\min_{0 \le k \le C-1} e^{(k)}$, where

$$e^{(k)} = \left| \mathbf{r}_P - \hat{\mathbf{r}}_P^{(k)} \right|^2. \tag{9}$$

As shown in Fig. 5, pilot symbol removal and FDE are performed following the pilot sequence identification. In this letter, the minimum mean square error (MMSE) equalizer is used where the equalization weights are given by $\zeta_m = \hat{f}_m^* / \left(\left| \hat{f}_m \right|^2 + \sigma_w^2 \right)$ for $0 \le m \le N-1$ and $\zeta_m = 0$ if $m \in I_P$. The estimated channel coefficients are given by $\hat{f}_m$. Flowcharts of the proposed transmission and reception algorithms are shown in Fig. 6.

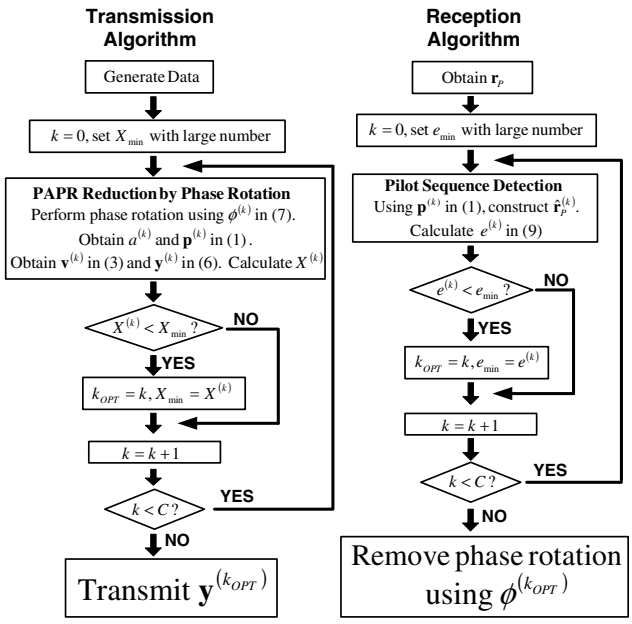

Fig. 6. Flowcharts of transmission and reception algorithms.

IV. SIMULATION RESULTS

The complementary cumulative distribution function (CCDF) of the PAPR, $P\left(X^{(k)} > \delta\right)$, of A-Hyb and FDSPT for quadrature phase shift keying (QPSK) and 64 quadrature amplitude modulation (QAM) are shown in Fig. 7 and 8 with $L_{OS} = 4$. As the performance benchmark, the CCDF performance of SC-OFDM with no pilot symbols is also shown in the figures. The parameters used in the simulation are set as $N = 256$, $N_T = 64$, $N_D = 96$, $N_{CP} = 16$ and $C = \{3, 5\}$. The normalized phase rotation angles $\phi^{(k)}$ and $a^{(k)}$ in (1) used for A-Hyb and FDSPT for $C = \{3, 5\}$ are summarized in Table I. From Fig. 7, it is clear that A-Hyb outperforms FDSPT by about 0.5 dB at CCDF$= 10^{-4}$ for QPSK. It is also observed that A-Hyb

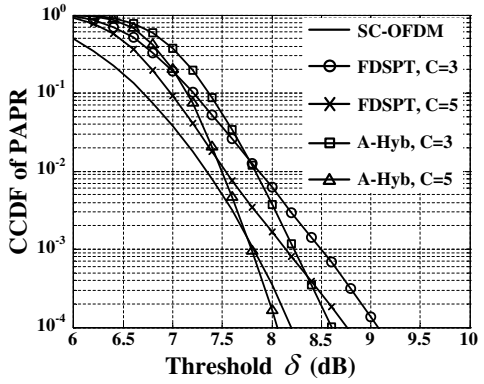

Fig. 7. PAPR Performance of A-Hyb and FDSPT for QPSK.

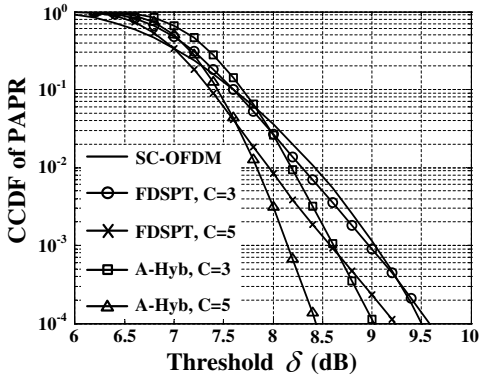

Fig. 8. PAPR Performance of A-Hyb and FDSPT for 64QAM.

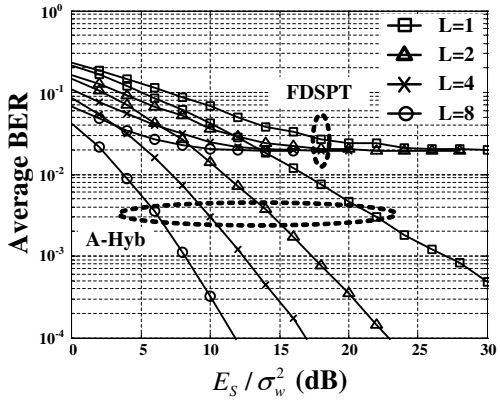

Fig. 9. BER Performance of A-Hyb and FDSPT for QPSK.

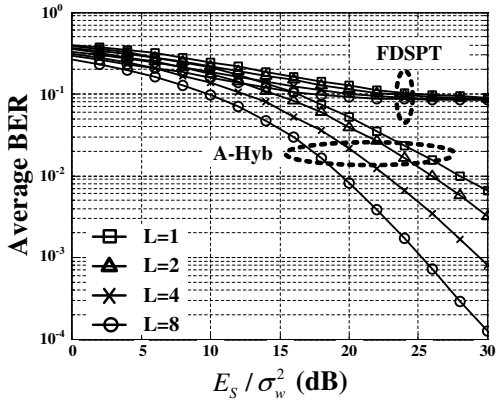

Fig. 10. BER Performance of A-Hyb and FDSPT for 64QAM.

yields similar PAPR performance as SC-OFDM when $C = 5$. From Fig. 8, it is clear that A-Hyb outperforms FDSPT by 0.8dB at CCDF= 10^{-4} for 64QAM when $C = 5$.

The uncoded average BER performances of A-Hyb and FDSPT in Rayleigh frequency selective channels with $C = 3$ for QPSK and 64QAM are presented in Fig. 9 and 10, respectively. The BER performance is plotted for different values of average signal to noise ratio (SNR) per symbol E_s/σ_w^2, where E_s indicates the energy per symbol. The iterative signal reconstruction scheme [7] with three iterations is applied to FDSPT. We consider Rayleigh frequency selective fading channels with $L = \{1, 2, 4, 8\}$ with the normalized Doppler frequency $f_D T_S = 2.7 \times 10^{-4}$. Linear interpolation is implemented to estimate CSI between four hybrid symbols with $T_D = 4$ and $F = 13$. In the simulation, we assume that nonlinearity due to a power amplifier is not present at the transmitter. From Fig. 9 and 10, it is clear that the proposed A-Hyb scheme outperforms FDSPT in all scenarios.

V. Conclusion

In this letter, a novel adaptive pilot insertion method for SC-OFDM systems to lower the PAPR was introduced. The simulation results have demonstrated that the proposed method outperforms the conventional method in both BER and PAPR performance.

VI. Acknowledgment

The authors would like to thank Dr. I. Chiba, Dr. M. Miyazaki, Dr. H. Sano and Dr. H. Nishimoto of Mitsubishi Electric Corporation for their encouragement and support throughout this work. The authors would also like to express sincere gratitude to the anonymous reviewers for their helpful suggestions.

References

[1] N. Benvenuto, R. Dinis, D. Falconer, and S. Tomasin, "Single carrier modulation with nonlinear frequency domain equalization: an idea whose time has come—again," *Proc. IEEE,* pp. 69–96, Jan. 2010.

[2] C.-T. Lam, D. D. Falconer, and F. Danilo-Lemoine, "PAPR reduction using frequency domain multiplexed pilot sequences," in *Proc. WCNC 2007*.

[3] D. Kim, U.-K. Kwon, and G.-H. Im, "Pilot position selection and detection for channel estimation of SC-FDE," *IEEE Commun. Lett.,* vol. 12, no. 5, pp. 350–352, May 2008.

[4] B. Sheng, X. Wang, X. You, and L. Chen, "A simple pilot position detection technique for channel estimation of SC-FDE," *IEEE Commun. Lett.,* vol. 14, no. 5, pp. 420–422, May 2010.

[5] D. Chu, "Polyphase codes with good periodic correlation properties," *IEEE Trans. Inf. Theory,* vol. 18, no. 4, pp. 531–532, July 1972.

[6] K. I. Ahmed, C. Tepedelenlioglu, and A. Spanias, "Performance of precoded OFDM with channel estimation error," *IEEE Trans. Signal Process.,* vol. 54, no. 3, pp. 1165–1170, Mar. 2006.

[7] U.-K. Kwon, D. Kim, and G.-H. Im, "Frequency domain pilot multiplexing technique for channel estimation of SC-FDE," *Electron. Lett.*, vol. 44, no. 5, pp. 364–365, Feb. 2008.